THE JOURNAL OF BIOLOGICAL CHEMISTRY
Vol. 277, No. 3, Issue of January 18, pp. 2321–2329, 2002
Printed in U.S.A.

The Cytoplasmic Tail of L-selectin Interacts with Members of the Ezrin-Radixin-Moesin (ERM) Family of Proteins

CELL ACTIVATION-DEPENDENT BINDING OF MOESIN BUT NOT EZRIN*

Received for publication, October 1, 2001
Published, JBC Papers in Press, November 8, 2001, DOI 10.1074/jbc.M109460200

Aleksandar Ivetic‡§, Jürgen Deka¶, Anne Ridley‖, and Ann Ager‡

From the ‡Divisions of Cellular Immunology and ¶Protein Structure, National Institute for Medical Research, The Ridgeway, Mill Hill, London NW7 1AA, ‖Ludwig Institute for Cancer Research, Royal Free and University College Medical School, 91 Riding House Street, London W1W 7BS, United Kingdom

L-selectin regulates the recruitment of naive lymphocytes from the bloodstream to secondary lymphoid organs, mediating their initial capture and subsequent rolling along high endothelial cell surface-expressed ligands in peripheral lymph nodes. *In vivo*, distribution of L-selectin and cell surface levels determine the tethering efficiency and rolling velocity of leukocytes, respectively. Treatment of naive lymphocytes with phorbol myristate acetate (PMA) induces rapid ectodomain proteolytic down-regulation (shedding) of surface L-selectin via a protein kinase C (PKC)-dependent pathway. In an attempt to isolate proteins that are involved in regulating L-selectin expression, an affinity column was constructed using the 17-amino acid cytoplasmic tail of L-selectin. Affinity purification of extracts from lymphocytes, pre-treated with or without PMA, allowed identification of proteins that interact with the affinity column under one condition but not the other. By using this approach, members of the Ezrin-Radixin-Moesin family of proteins were found to interact specifically with the cytoplasmic tail of L-selectin. Moesin from PMA-stimulated lymphocytes, but not from unstimulated lymphocytes, bound to L-selectin tail. In contrast, ezrin from unstimulated or PMA-stimulated lymphocytes associated with L-selectin tail with equal affinity. Furthermore, the PKC inhibitor Ro 31-8220 significantly reduced the interaction of moesin, but not ezrin, with L-selectin. Alanine mutations of membrane-proximal basic amino acid residues in the cytoplasmic domain of L-selectin identified arginine 357 as a critical residue for both ezrin and moesin interaction. Finally, BIAcore affinity analysis confirmed that N-terminal moesin interacts specifically with L-selectin cytoplasmic tail, with relatively high affinity (K_d ≈40 nM). Based on these findings, although moesin and ezrin bind to a similar region of the cytoplasmic tail of L-selectin, moesin binding is dependent on PKC activation, which suggests that ezrin and moesin are regulated differently in lymphocytes.

L-selectin is a member of the selectin family of cell adhesion molecules that is expressed exclusively on leukocytes. L-selectin is a type I transmembrane glycoprotein composed of a C-type calcium-dependent lectin domain, an epidermal growth factor-like domain, two short consensus repeats, a membrane-proximal cleavage site, a transmembrane domain, and a short 17-amino acid cytoplasmic tail (1) (see Fig. 1*A*). L-selectin is directly involved in the primary steps of leukocyte recruitment, where leukocytes tether and subsequently roll along mucin-like endothelial cell ligands (2). Regulation of L-selectin expression is poorly understood; however, recent studies on the cytoplasmic tail of L-selectin have implicated its role in regulating cell surface levels and localization on the cell membrane.

The membrane-proximal and membrane-distal domains of L-selectin cytoplasmic tail have been reported to independently regulate L-selectin surface expression and function, respectively. The membrane-distal region of L-selectin has been shown to interact with the cytoskeletal protein, α-actinin (3). Truncation of the C-terminal 11 amino acids of human L-selectin (known as LΔcyto) abrogates interaction with α-actinin. Although carbohydrate ligand binding remains unaltered, 300.1 pre-B cells expressing LΔcyto cannot adhere to high endothelial venules (derived from *in vitro* frozen section assays) or roll along L-selectin ligands (4). Antibody- or ligand-mediated cross-linking of wild-type L-selectin, but not LΔcyto, promotes associations with the actin-based cytoskeleton, demonstrating that the membrane-distal domain of L-selectin mediates interactions with the cytoskeleton and plays a role in L-selectin avidity (5). Electron microscopic analysis clearly demonstrates normal distribution of LΔcyto on microvilli of 300.1 pre-B cells (3), suggesting that the remaining membrane-proximal six amino acids (RRLKKG) are involved in anchoring L-selectin to microvilli. Cytoplasmic and transmembrane domain-swap experiments between L-selectin and CD31/CD44 reveal that localization of L-selectin on microvilli plays an important role in the initial capture (or tethering) of leukocytes to the endothelium (6), which is the first characterized stage of the "multistep adhesion cascade" (7). The membrane-proximal cytoplasmic domain of L-selectin has been shown to interact with calmodulin, in a calcium-independent manner, and point mutations L358E and K359E (in L-selectin) prevent this interaction (8). In resting human neutrophils, constitutive association of calmodulin with the cytoplasmic tail of L-selectin is thought to alter the topology of the extracellular membrane-proximal cleavage domain of L-selectin, rendering it resistant to proteolysis. PMA[1] stimulation, or incubation with calmodu-

* This work was supported by the Medical Research Council (United Kingdom) and by European Union Grant CT-1999-01036. The costs of publication of this article were defrayed in part by the payment of page charges. This article must therefore be hereby marked "*advertisement*" in accordance with 18 U.S.C. Section 1734 solely to indicate this fact.

§ To whom correspondence should be addressed: Ludwig Institute for Cancer Research, 91 Riding House St., London W1W 7BS, United Kingdom. Tel.: 00-44-20-7878-4000; Fax: 00-44-20-7878-4040.

[1] The abbreviations used are: PMA, phorbol myristate acetate; PKC, protein kinase C; ERM, Ezrin-Radixin-Moesin; BSA, bovine serum albumin; MALDI, matrix-assisted laser desorption ionization; PBS, phosphate-buffered saline; Tricine, *N*-[2-hydroxy-1,1-bis(hydroxymethyl) ethyl]glycine; CPERM, C-terminally phosphorylated ERM proteins; EF-1α, elongation factor 1α; ABC, ammonium bicarbonate.

lin antagonists, releases calmodulin from L-selectin cytoplasmic tail and results in L-selectin shedding. Therefore, the release of calmodulin from L-selectin is assumed to alter the topology of the cleavage domain, permitting it to be cleaved. Calmodulin antagonists have been shown more recently to induce the shedding of other transmembrane proteins, suggesting that this mechanism is not specific to L-selectin (9).

We have developed a method for analyzing intracellular proteins that interact with the cytoplasmic tail of L-selectin (Fig. 1*B*). By using affinity purification chromatography, we demonstrate that the cytoplasmic tail of L-selectin interacts with members of the Ezrin-Radixin-Moesin (ERM) family of proteins (10). Ezrin can associate constitutively with L-selectin tail, whereas moesin only associates with L-selectin tail under PMA-stimulating conditions. Alanine mutation analysis of the membrane-proximal region of L-selectin cytoplasmic tail demonstrates that R357A is critical for both moesin and ezrin interaction. In addition we show that treatment of lymphocytes with the PKC inhibitor, Ro 31-8220, significantly reduces the interaction of moesin, but not ezrin, with L-selectin. Finally, we demonstrate specific interactions between purified N-terminal moesin and L-selectin tail to be specific, as measured by BIAcore affinity analysis ($K_d \approx 40$ nm). We discuss the differing roles that ezrin and moesin may have with respect to L-selectin surface expression/localization on naive lymphocytes.

EXPERIMENTAL PROCEDURES

Materials—Unless otherwise stated, all chemicals were purchased from Sigma.

Cells and Antibodies—Naive murine lymphocytes were isolated as described previously (11). Lymphocytes were obtained from pooled axilliary, cervical, and mesenteric lymph nodes or spleens of 6–8-week-old BALB/c mice. The following antibodies were obtained from the various suppliers indicated in parentheses: anti-human HMG-1 (rabbit polyclonal, PharMingen); anti-human moesin and ezrin (goat polyclonal, Santa Cruz Biotechnology); anti-human EF-1α (mouse monoclonal, Upstate Biotechnology, Inc.); anti-murine CPERM (mouse monoclonal 297S, kind gift from S. Tsukita, Kyoto Japan); anti-bovine calmodulin (mouse monoclonal, kind gift from D. Sacks).

Immunoblotting and SDS-PAGE—All protein samples were resolved using 4–12% gradient Bis-Tricine-SDS-polyacrylamide gels (NOVEX/Invitrogen). Further resolution of ezrin and moesin was performed using 3–8% gradient Tris acetate gels (NOVEX/Invitrogen). Polyacrylamide gels were either transferred to nitrocellulose or silver-stained (Bio-Rad silver stain Plus kit), according to manufacturers' instructions. All proteins were transferred onto PVDF membrane (Immobilon-P) at a constant 25 V for approximately 1 h, using a pre-prepared transfer buffer system that contained 10% methanol (NOVEX/Invitrogen). Calmodulin was detected following pretreatment of PVDF membrane with PBS containing 2.5% (v/v) glutaraldehyde (to chemically cross-link transferred proteins to the membrane) for 45 min, prior to incubation with blocking solution (5% (w/v) powdered milk (Marvel) in PBS). Incubation with ~1 μg/ml primary antibody (diluted in blocking solution) was performed routinely at room temperature for 1 h (or overnight at 4 °C) with gentle agitation. Anti-CPERM antibodies were used neat as tissue culture supernatant. Prior to the addition of secondary antibody, filters were washed 2 times for 7 min in PBS containing 0.1% (v/v) Nonidet P-40, followed by a single wash for 7 min in PBS. To reduce background signal, all filters were blocked in blocking solution for a further 45 min prior to the addition of secondary antibody. All secondary antibodies for Western blotting (*i.e.* rabbit anti-goat, rabbit anti-mouse, and swine anti-rabbit) were purchased from DAKO as horseradish peroxidase conjugates and used routinely at a dilution of 1:3,000 in blocking solution and used at similar incubation conditions as for primary antibody. Filters were washed as described above prior to addition of ECL chemiluminescent substrate (Amersham Biosciences) and exposed to x-ray film (Eastman Kodak Co.) according to the manufacturers' instructions.

Construction of Affinity and Scrambled Peptide Columns—Peptides were synthesized using an Applied Biosystems 430A peptide synthesizer and purified by reverse phase high pressure liquid chromatography. Peptide purity was assessed by mass spectroscopy and high pressure liquid chromatography. All peptides used in this report are listed in Table I.

1 and 5 ml of Hi-Trap *N*-hydroxysuccinimide-activated Sepharose columns (Amersham Biosciences) were used for the construction of affinity, alanine-mutated, and scrambled peptide columns. Peptides were coupled to *N*-hydroxysuccinimide-activated Sepharose, and coupling efficiency was monitored according the manufacturers' protocol. Columns were washed in calcium and magnesium free PBS containing 0.2% (w/v) NaN_3 and stored at 4 °C. Depending on the affinity purification procedure, scrambled, mutated, and affinity columns were stacked on top of each other (see Fig. 1*B*). This construction minimized the time required for cell extracts flowing through the scrambled peptide column to be transferred to either mutant and (or) affinity columns.

Affinity Purification Procedure—For every affinity purification procedure ~2×10^8 lymphocytes were harvested and washed in ice-cold calcium and magnesium-free PBS. Cells were resuspended in 15 ml of RPMI 1640 (Invitrogen) containing 1% (v/v) fetal calf serum, in the absence or presence of 500 nM PMA, and incubated at 37 °C for 15 min (with occasional swirling to prevent cells from settling). In some experiments, cells were preincubated with 1 μM of the PKC inhibitor Ro 31-8220 for 20 min at 37 °C, prior to stimulation with PMA. After stimulation, cells were harvested by centrifugation and lysed using 5 ml of lysis buffer (25 mM HEPES (pH 7.4); 150 mM NaCl; 1% (v/v) Nonidet P-40; 1 mM sodium pervanadate; 2 mM EDTA) in Complete™ protease inhibitor mixture (Roche Molecular Biochemicals). Cell lysates were left on ice for 30 min and subsequently clarified by micro-centrifugation at 13,000 × *g* at 4 °C. Supernatants were diluted 10 times using buffer A (25 mM HEPES (pH 7.4); 50 mM NaCl; 5% (v/v) glycerol; 1 mM sodium pervanadate; 2 mM EDTA containing Complete™ protease inhibitor mixture). The entire diluted supernatant was applied to the column construct (pre-equilibrated in buffer A) (Fig. 1*B, step 1*), followed by a thorough wash of at least 10 column volumes of buffer A (Fig. 1*B, step 2*). The scrambled peptide column and the affinity column were subsequently detached from one another. The affinity column was subjected to sequential increasing concentrations of NaCl in buffer A (*i.e.* 100, 250, and 500 mM and 1 M NaCl) (Fig. 1*B, step 3*). Any bound material remaining on the affinity column after the 1 M NaCl wash was eluted using an ethanolamine-based elution buffer (0.5 M NaCl; 0.5 M ethanolamine (pH 8.0)). The scrambled and mutant peptide columns were subjected to a single elution step using ethanolamine-based elution buffer (Fig. 1*B, step 4*). All elutions were resolved by SDS-PAGE and silver-stained for analysis. Protein bands of interest were excised for mass spectrometric analysis (Fig. 1*B, step 5*).

Tryptic In-gel Digestion of Proteins Resolved by One-dimensional SDS-PAGE—Following silver stain analysis, fractions containing proteins of interest were resolved by SDS-PAGE and stained with colloidal Coomassie (Invitrogen/NOVEX), according to the manufacturer's protocol. Protein bands of interest were identified, excised with a sterile razor, and placed in a 0.5-ml Treff (Scotlab) tube. SDS and Coomassie were removed by incubating the gel slice three times with 500 μl of wash buffer containing 200 mM ammonium bicarbonate (ABC), 50% (v/v) acetonitrile for 30 min at 30 °C. The gel slice was reduced with 200 μl of reducing buffer (20 mM dithiothreitol, 200 mM ABC, 50% (v/v) acetonitrile) for 1 h at 30 °C and then washed four times in wash buffer. Cystines were subsequently alkylated with freshly prepared alkylating buffer (5 mM iodoacetamide, 200 mM ABC, 50% (v/v) acetonitrile) for 20 min in darkness at room temperature. The gel slice was washed four times in a modified wash buffer (50% (v/v) acetonitrile, 20 mM ABC) and then incubated in 500 μl of neat acetonitrile for 15 min. The gel slice was subsequently dried in a vacuum centrifuge, re-hydrated in 30 μl of 5 mM ABC containing ~60 ng of methylated porcine trypsin (Promega), and allowed to digest for 16–24 h at 37 °C. Digested samples were subsequently analyzed by MALDI-mass spectrometry.

BIAcore Affinity Analysis—Human N-terminal moesin (residues 1–297) was overexpressed and purified according to a protocol published previously (12) (The expression plasmid encoding the open reading frame of N-terminal moesin was a kind gift from A. Bretscher, Cornell, NY). Association and dissociation reactions involving N-terminal moesin and biotinylated L-selectin cytoplasmic tail were studied by surface plasmon resonance in a BIAcore system (BIAcore AB, Uppsala, Sweden). The general principles of this method were reviewed recently (13). To avoid covalent inactivation of essential side chains, the cytoplasmic tail of L-selectin was synthesized as a biotinylated peptide (conjugated to Arg-356) and immobilized on the sensor surface using a non-covalent sandwich system. The peptide was coupled via the N-terminal biotin moiety to streptavidin-coated sensorchip (sensorchip SA BIAcore AB).

For the analysis of the interaction between the N-terminal domain of human moesin and immobilized L-selectin peptide, purified N-terminal moesin was injected at different concentrations in 10 mM HEPES (pH

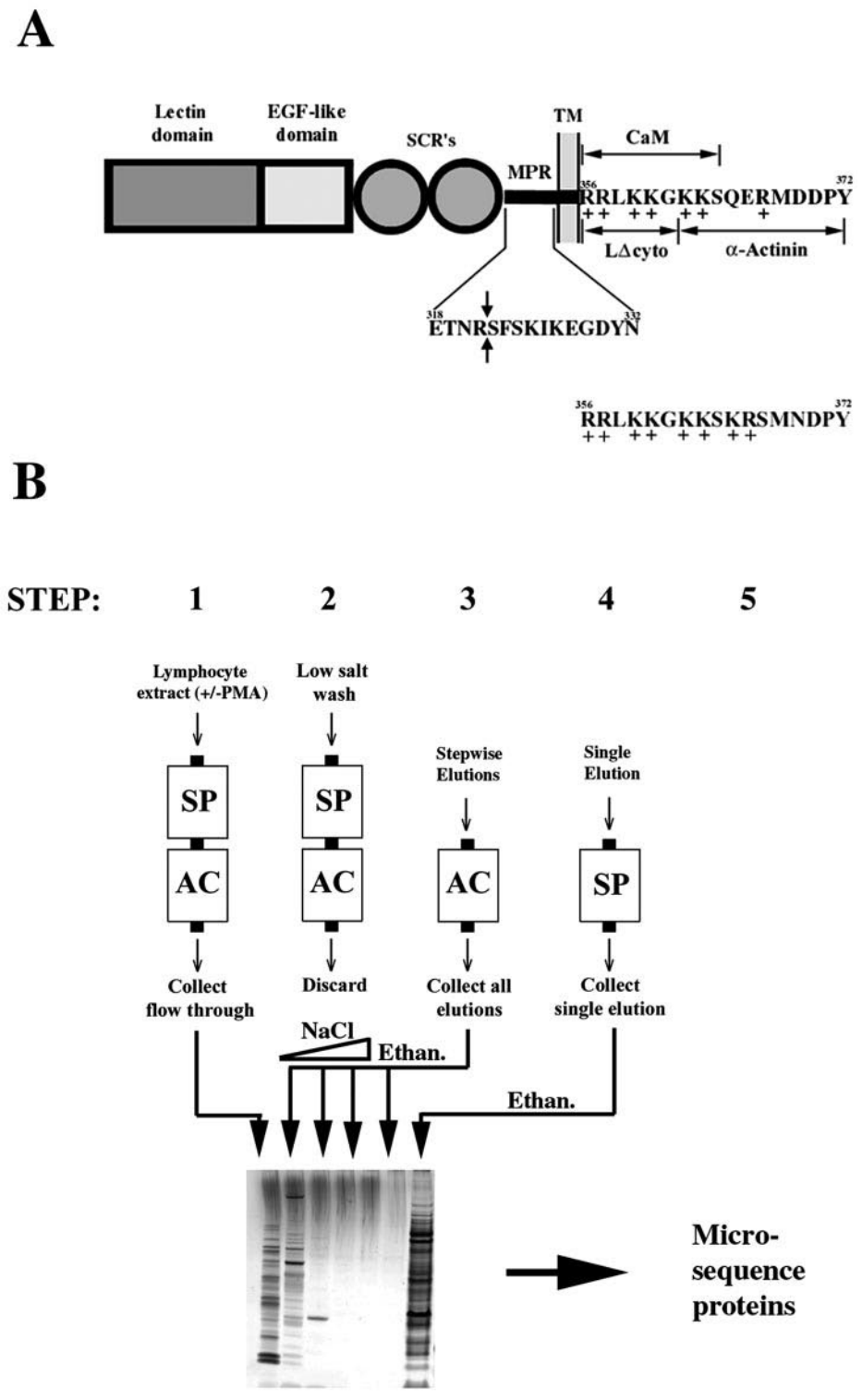

FIG. 1. **Schematic representation of murine L-selectin, displaying amino acids for the membrane-proximal region and cytoplasmic tail and a 5-step schematic representation for affinity-purifying extracts derived from untreated (−) or PMA-stimulated (+) lymphocytes.** *A, EGF,* epidermal growth factor; *SCR,* short consensus repeat; *MPR,* membrane-proximal region; *TM*, transmembrane domain. Amino acid numbers are indicated for the cytoplasmic tail and the membrane-proximal region sequences. *Black inward-facing arrows above* and *below* the membrane-proximal region amino acid sequence indicate the putative cleavage site (*i.e.* between Arg-321 and Ser-322). Positively charged residues present in L-selectin cytoplasmic tail are indicated with a +. *LΔcyto* indicates the amino acids remaining in the cytoplasmic tail after truncation of the C-terminal 11 amino acids (considered the α-actinin-binding domain). The putative calmodulin (*CaM*) and α-actinin-binding sites are indicated. The cytoplasmic tail of human L-selectin is shown on the *bottom right-hand side* of this figure. Human and murine L-selectin cytoplasmic tails are 100% conserved between residues Arg-356 and Ser-364. *B,* stepwise increases in NaCl concentration were used to elute and thus fractionate proteins interacting with the affinity column (*AC*) (100, 250, 500 mM, 1 M). An ethanolamine-based elution buffer (*Ethan.*, see "Experimental Procedures") was used to elute the contents of the affinity column following a final 1 M NaCl wash. The entire contents of the scrambled peptide column (*SP*) was obtained in a single elution, using an ethanolamine-based buffer. All fractions were resolved on the same polyacrylamide gel and stained with colloidal Coomassie SDS-PAGE. Bands of interest were identified, excised, and trypsinized for subsequent microsequencing by MALDI-mass spectrometry.

7.4), 150 mM NaCl, 0.005% (v/v) polysorbate 20 (HSP-P, BIAcore AB) with a flow rate of 5 μl/min. The binding and K_d values were analyzed by monitoring the optical resonance from the injection start time. The dissociation reaction was monitored while flushing the L-selectin-moesin complex with HBS-P. Data were evaluated using the BIAevaluation software (version 3.0.2). Regeneration of the sensor surface was achieved by injection of 100 mM NaOH followed by subsequent reloading of the sensor surface with 1 μM biotinylated L-selectin cytoplasmic tail. All measurements were monitored at 25 °C.

RESULTS

Affinity Chromatography of Extracts Prepared from Lymphocytes Pre-treated with or without PMA—A peptide comprising the short cytoplasmic tail of L-selectin was synthesized and used to construct an affinity column (see "Experimental Procedures"). The 17 amino acids that constitute the cytoplasmic tail of L-selectin contribute to an overall pI of ~10.2 (Fig. 1*B*). Producing an affinity column with relatively high basicity could prove problematic because of nonspecific interactions with proteins derived from cell extracts. This problem was circumvented by synthesizing a peptide (with a similar pI) containing a scrambled sequence of the cytoplasmic tail (chosen randomly) and immobilizing it onto a similar support (Table I). The scrambled peptide column was assembled on top of the

TABLE I
A list of peptides synthesized for affinity chromatography and BIAcore affinity experiments

Peptide (name)	Species origin	Modifications
EGRMKQPDKRDSKYKRL (Scram)	Murine	None
RRLKKGKKSQERMDDPY (WT)	Murine	None
Bio-RRLKKGKKSQERMDDPY (WT)	Murine	N-terminal biotinylated
RALKKGKKSKRSMNDPY (R357A)	Human	None
RRLKAGKKSKRSMNDPY (K360A)	Human	None
RRLKKGKASKRSMNDPY (K363A)	Human	None

affinity column and served to pre-clear extracts of any nonspecifically interacting proteins (Fig. 1*B, step 1*). By using this approach, unbound material leaving the scrambled column immediately entered the affinity column, minimizing the requirement for transfer steps. After the cell extract had passed through the column construct, a thorough low salt wash (at least 10 column volumes of wash buffer containing 50 mM NaCl) followed to remove any unbound material (Fig. 1*B, step 2*). Prior to fractionation the column construct was unassembled and the affinity column was subjected to a stepwise non-linear series of elutions with increasing NaCl concentration (*i.e.* 100, 250, and 500 mM and 1 M NaCl), followed by a final elution step, using an ethanolamine-based elution buffer to remove any bound material (Fig. 1*B, step 3*). The entire contents of the scrambled peptide column was subjected to a single elution step using an ethanolamine-based elution buffer (Fig. 1*B*, *step 4*). Eluates from the affinity column were collected and resolved by SDS-PAGE.

Extracts derived from untreated and PMA-stimulated lymphocytes were individually fractionated on the affinity column. The elution profile of each fractionated extract was determined by SDS-PAGE and subsequent silver staining (Fig. 2). This procedure facilitated identification of proteins interacting with the cytoplasmic tail of L-selectin primarily under PMA-stimulating conditions. The majority of proteins in extracts from untreated and PMA-activated lymphocytes eluted from the affinity column at 100 mM NaCl, giving rise to ~15 protein bands (Fig. 2, *A* and *B, lanes 3–5*). Fractionation of extracts derived from untreated or PMA-stimulated lymphocytes (overall) produced different elution profiles. The most obvious differences between the two fractionated extracts occurred at the 250 and 500 mM NaCl elutions. At these NaCl concentrations, some protein bands were visible only in extracts fractionated from PMA-stimulated lymphocytes (Fig. 2 compare *A* and *B, lanes 8–10* and *13–15*). Differences in elution profiles were also observed at 1 M NaCl (Fig. 2, compare *A* and *B, lanes 17–20*).

Identification of Proteins Derived from PMA-stimulated Lymphocyte Extracts, Eluting from L-selectin Affinity Column—Because our main interest was to identify proteins from PMA-stimulated cells that associate with the cytoplasmic tail of L-selectin, we focused on obtaining microsequences of proteins fractionated from lymphocytes that were stimulated with PMA. Fractions containing the protein bands of interest (Fig. 2*B*, see *asterisks*) were resolved by SDS-PAGE, identified with colloidal Coomassie Blue staining (NOVEX/Invitrogen), and excised for microsequencing by MALDI-mass spectrometry. Of the four proteins excised from colloidal Coomassie-stained polyacrylamide gels, amino acid sequences were obtained from three bands (see Table II). The proteins identified were moesin (Fig. 2*B, lane 8*, ~70 kDa), Elongation Factor 1α (EF-1α) (Fig. 2*B, lane 18, upper band,* ~52 kDa) and HMG-1 (Fig. 2*B, lane 18, lower band*, ~30 kDa). Antibodies directed against the three proteins were used for immunoblotting and verified the identity of all three proteins and, in parallel, assessed whether they specifically bound to the affinity column or not (Fig. 3). Both moesin and HMG-1 eluted specifically from the affinity column, and not the scrambled peptide column, at 100 and 500 mM NaCl, respectively (Fig. 3*A, upper* and *middle blots*, compare *lanes 1* and *3* with *lane 6*). EF-1α was shown to interact with the scrambled peptide column (Fig. 3*A, lower blot, lane 6*) and was therefore considered to interact nonspecifically with the affinity column. Although we observe EF-1α eluting from the affinity column, immunoblotting clearly demonstrated a greater amount of this protein binding to the scrambled peptide column.

We next analyzed the same fractionated cell extracts to determine whether ezrin, another member of the ERM family of proteins, was interacting with the affinity column. Immunoblotting with anti-ezrin polyclonal antibody detected ezrin in the 100 mM NaCl fraction (Fig. 3*B, upper blot, lane 1*), and as with moesin, ezrin did not bind to the scrambled peptide column (Fig. 3*B, upper blot, lane 6*). These results indicate that both ezrin and moesin bound specifically to the cytoplasmic tail of L-selectin. Under slightly altered wash conditions (*i.e.* using 100 mM NaCl instead of using 50 mM NaCl), we found calmodulin associating with the affinity column and eluting at 250 mM NaCl (Fig. 3*B, lower blot, lane 2*). The relatively acidic nature of calmodulin meant that at 50 mM NaCl wash conditions calmodulin would associate with the scrambled peptide column (data not shown). Our data demonstrate that this approach has led to the identification of novel L-selectin tail-interacting proteins, as well as validating this approach by identifying a protein previously reported to interact with L-selectin tail (*i.e.* calmodulin).

PMA Stimulation Regulates Recruitment of Moesin, but Not Ezrin, to the Cytoplasmic Tail of L-selectin—Comparison of anti-moesin and anti-ezrin immunoblots of extracts fractionated from untreated and PMA-stimulated lymphocytes revealed that moesin interacts with L-selectin only under PMA-stimulating conditions (Fig. 4*A*), whereas ezrin interacts with L-selectin tail irrespective of pre-treatment of lymphocytes with PMA (Fig. 4*B*). We next assessed whether Ro 31-8220, an inhibitor of all known PKC isoforms, could inhibit PMA-induced recruitment of moesin to the cytoplasmic tail of L-selectin. Lymphocytes were pre-treated with or without 1 μM Ro 31-8220 and subsequently stimulated with PMA as before. Extracts fractionated from each lymphocyte preparation revealed that Ro 31-8220 considerably reduced the interaction of moesin with L-selectin cytoplasmic tail affinity column (Fig. 4*C, upper blot*, compare *lane 1* with *2*). The interaction of ezrin with the affinity column, however, remained unaffected by this treatment (Fig. 4*C, bottom blot,* compare *lane 1* with *2*). These results indicate that the PMA-induced recruitment of moesin to the cytoplasmic tail of L-selectin is dependent on PKC activity. Interestingly, immunoblotting of crude extracts of lymphocytes using the monoclonal antibody 297S (which detects the presence of C-terminal threonine-phosphorylated ERM proteins) detected no difference in the levels of phosphorylated ezrin or moesin in the presence or absence of PMA (Fig. 4*D*, compare *lanes 1* and *3*). The lysis conditions used in these procedures liberated all detectable activated moesin and ezrin into the soluble, rather than the insoluble, fraction of the lysates (Fig. 4*D*, compare *lanes 1* and *3* with *lanes 2* and *4*).

Specific Enrichment of C-terminally Phosphorylated ERM Proteins by L-selectin Tail—Activated ERM proteins are generally considered to interact with type I integral membrane proteins via their N terminus and with F-actin via their C terminus, which is how they cross-link cell adhesion molecules with the actin-based cortical cytoskeleton (14). Ezrin, radixin, and moesin become activated upon phosphorylation of C-terminal threonine 567, 564, and 558, respectively, which disrupts

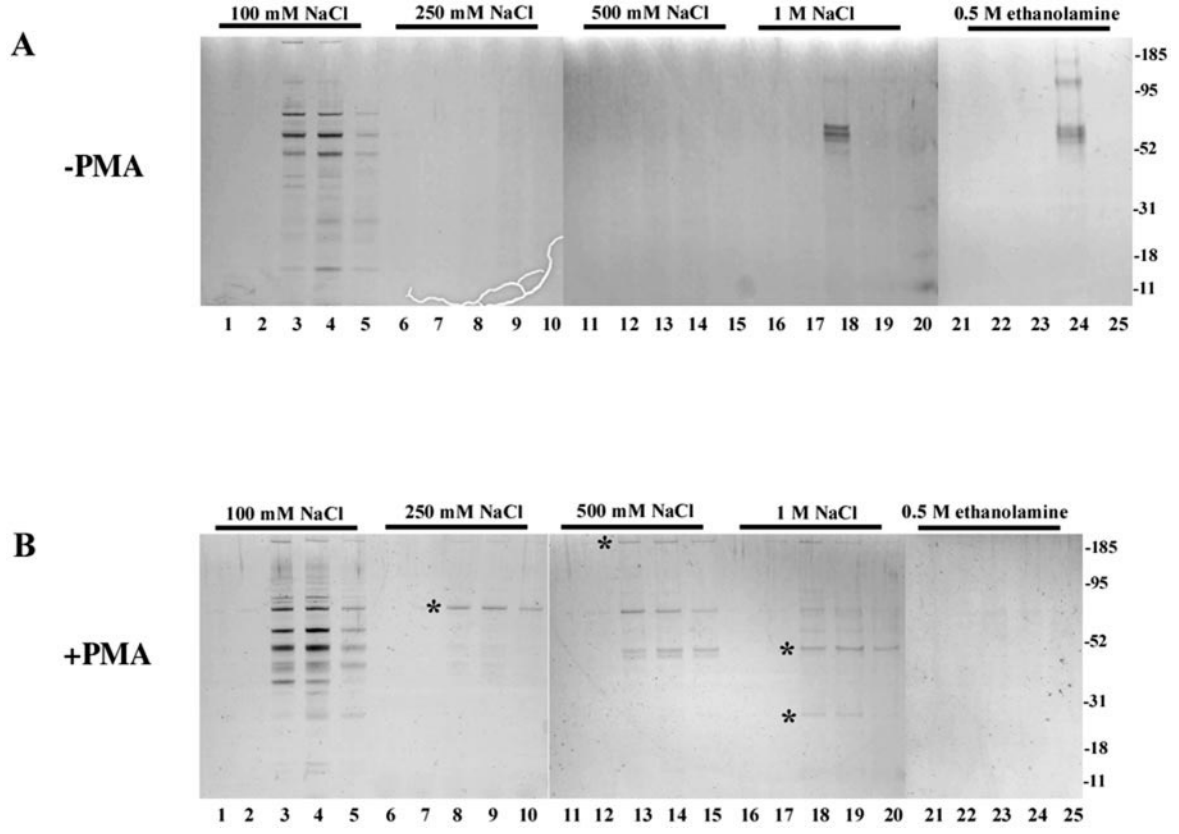

FIG. 2. **Silver-stained elution profiles of affinity-purified extracts derived from untreated/PMA-stimulated lymphocytes.** Each NaCl and ethanolamine-based elution contains the first five fractions eluting from the affinity column only. *Asterisks* denote the proteins that were subsequently excised from the polyacrylamide gel and subjected to MALDI-mass spectroscopy. Molecular mass standards are indicated in kilodaltons.

TABLE II
Amino acid sequences derived from gel-purified, trypsin-digested fragments identified by MALDI mass spectroscopy

Size of protein	Peptides identified	Name of protein (GenBank™ accession number)
30 kDa	HPDASVNFSEFSK PKIKGEHPGLSIGDVAKK LKEKYEKDIAAYR YYVTIIDAPGHR QLIVGVNKMDSTEPPYSQKR	**HMG-1 (L38477)**
52 kDa	IGGIGTVPVGR RGNVAGDSK FAVRDMR SGYLAGDKLLPQR LNKDQWEER KAPDFVFYAPR RKPDTIEVQQMK	**EF-1α (M22432)**
70 kDa	AQQELEEQTRRALELEQER QEAEEAKEALLQASR KTQEQLASEMAELTARISQLEMAR ESEAVEWQQK DRSEEERTTEAEKNER ALTSELANARDESK QRIDEFESM	**Moesin (P26041)**

intramolecular associations between the N and C termini (15). Monoclonal antibody 297S, which is specific for the C-terminally phosphorylated ERM proteins (CPERM), detected an enrichment of CPERM in fractions specifically eluting from the affinity column (Fig. 5*C, lane 4*). This demonstrates that some, if not all, of the ERM proteins interacting with the affinity column are in an activated, phosphorylated form. During occasional purification procedures, we detected ezrin binding to the scrambled peptide column (Fig. 5*A, lane 3*). This form of ezrin was not detected by monoclonal antibody 297S (Fig. 5*C, lane 3*) and is therefore considered to be inactivated and is interacting nonspecifically with the scrambled peptide column. It is interesting to note that the relative amount of CPERM proteins present in lymphocyte extracts (or the "load") is negligible with respect to the total amount of moesin and ezrin detected by the anti-moesin and anti-ezrin polyclonal antibodies (Fig. 5, compare *lane 1* in *A–C*), clearly demonstrating that the affinity column can specifically enrich for CPERM proteins.

Arginine 357 Is Essential for Ezrin and Moesin Interaction with L-selectin—Previous reports (16, 17) have demonstrated the binding of ERM proteins to charged clusters of basic amino acids residing on membrane-proximal cytoplasmic tails of cell adhesion molecules. L-selectin carries three sets of di-basic residues along its cytoplasmic tail. Single alanine mutations were introduced into one of the two basic residues along the cytoplasmic tail to address whether such mutations would impair ERM binding. Peptides were synthesized and used to construct alanine mutant peptide affinity columns (Table I). The mutant peptide column was introduced between the scrambled peptide column and the affinity column (Fig. 6). Proteins unable to bind to an L-selectin tail mutant would pass through the mutated peptide column and subsequently bind to the affinity column. Proteins unaffected by the mutation would bind directly to the mutated peptide column and not the affinity column. Both ezrin and moesin were unable to bind to the R357A mutant peptide column and interacted exclusively with the affinity column containing the wild-type peptide sequence (Fig. 6*A*). The mutations K360A and K363A did not appear to abrogate the binding of either ezrin or moesin to the L-selectin tail (Fig. 6, *B* and *C*, respectively).

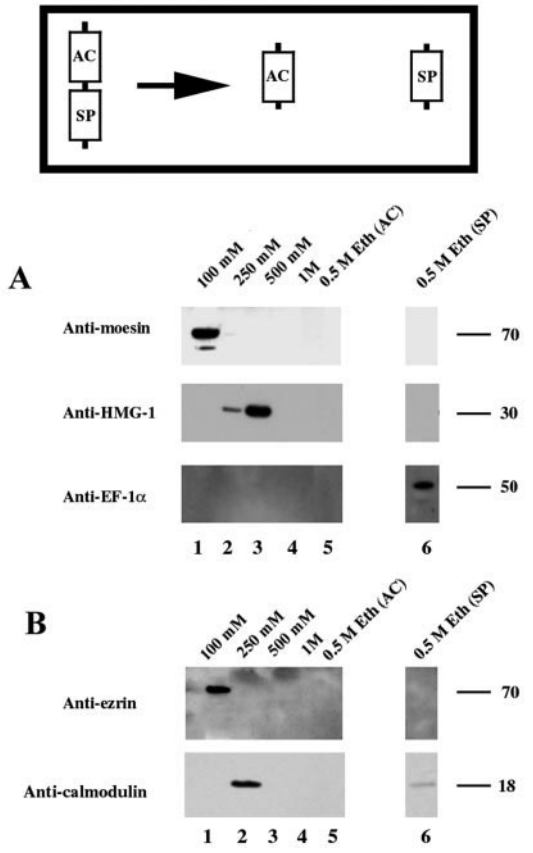

FIG. 3. **Immunoblot analysis of proteins identified by MALDI-mass spectrometry.** *Schematic* at the *top* of the figure represents the order in which the columns were arranged and detached for subsequent elution. Extracts derived from PMA-stimulated lymphocytes were fractionated on the affinity and scrambled column construct. *A,* fractions eluting from the affinity column (*AC*) and/or the scrambled peptide column (*SP*) were Western-blotted with antibodies against moesin (*upper blot*), HMG-1 (*middle blot*), and EF-1α (*lower blot*). A possible degradation product is detected for moesin (less intense, faster migrating band in *lane 1*, *upper blot*). *B,* anti-ezrin immunoblot analysis of the same fractions revealed that ezrin also associates specifically with the affinity column (*upper immunoblot*). Under 100 mM NaCl wash conditions, calmodulin was found to elute from the affinity column at 250 mM NaCl (*lower immunoblot*).

Direct Interaction between the N-terminal Domain of Moesin and L-selectin Tail Using BIAcore Affinity Analysis—BIAcore surface plasmon resonance technology allowed monitoring of interactions between soluble recombinant N-terminal moesin (amino acids 1–297) and L-selectin tail. Biotinylated L-selectin cytoplasmic tail was immobilized to a sensorchip which itself was precoated with streptavidin. Both N-terminal moesin and BSA were monitored for their ability to interact with L-selectin cytoplasmic tail. Analysis of the sensorgrams demonstrated that N-terminal moesin, but not BSA, was able to bind to immobilized L-selectin (Fig. 7*A*). Both BSA and N-terminal moesin displayed negligible binding to BIAcore streptavidin-coated sensor chips (data not shown). To address the specificity of interaction, 100 μM of either soluble L-selectin cytoplasmic tail or scrambled peptides were used to compete off N-terminal moesin, pre-loaded onto immobilized L-selectin cytoplasmic tail. Competition studies clearly demonstrate that N-terminal moesin can be specifically competed off using soluble L-selectin cytoplasmic tail but not with the scrambled peptide (Fig. 7*B*). Finally, we determined the dissociation constant (K_d) of the interaction between N-terminal moesin and L-selectin cytoplasmic tail to be ~40 nM (Fig. 7*C*). These results support the evidence that both L-selectin and moesin interact specifically.

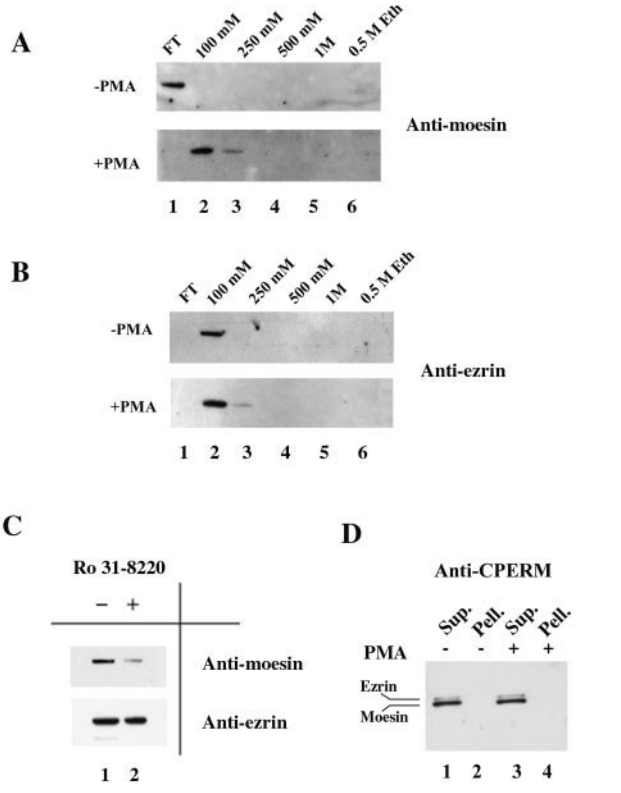

FIG. 4. **The recruitment of moesin, but not ezrin, to the cytoplasmic tail of L-selectin is regulated by PMA stimulation and sensitive to PKC inhibitor Ro 31-8220.** *A,* anti-moesin antibody detects moesin in the flow-through (*FT*) using untreated lymphocyte extracts (−*PMA*) and in the 100 mM NaCl fraction using PMA-stimulated lymphocyte extracts (+*PMA*). *B,* anti-ezrin polyclonal antibody detects ezrin from both untreated (−*PMA*) and PMA-treated (+*PMA*) lymphocyte extracts interacting with the affinity column. *C,* lymphocytes were pre-treated with (+) or without (−) 1 μM of the PKC inhibitor Ro 31-8220 for 20 min at 37 °C and subsequently stimulated with 500 nM PMA, prior to affinity purification on L-selectin tail affinity column. Extracts were applied to a column construct containing the scrambled peptide stacked on top of the wild-type L-selectin tail column and washed extensively in 50 mM NaCl wash buffer. The columns were subsequently detached, and the affinity column was eluted using ethanolamine (*Eth*)-based elution buffer. Anti-moesin and anti-ezrin immunoblots detected the relative abundance of moesin and ezrin associated with the affinity column from each treatment. *D,* equal numbers of lymphocytes were treated with or without 500 nM PMA and subsequently lysed in lysis buffer. Lysates were centrifuged for 15 min (see "Experimental Procedures"). Supernatant (*Sup.*) and pellet (*Pell.*) fractions were resolved on 3–8% Tris acetate gels, transferred to nitrocellulose, and probed with monoclonal antibody 297S (*anti-CPERM*). Levels of C-terminally phosphorylated ezrin and moesin were detected exclusively in the supernatant fraction of lymphocyte lysates and did not appear to differ in the presence or absence of PMA stimulation.

DISCUSSION

We have used affinity chromatography as a method to isolate intracellular proteins that interact with the cytoplasmic domain of L-selectin from PMA-stimulated lymphocytes. By using this approach, we identified two members of the highly related ERM family of proteins, moesin and ezrin, and the nuclear/extracellular protein HMG-1/amphoterin (18, 19) interacting with L-selectin cytoplasmic tail. We also identified calmodulin interacting with L-selectin tail, which supports the previous finding (8) that calmodulin interacts with human L-selectin tail and validates this approach. This is the first report demonstrating interactions between the ERM family of proteins and L-selectin cytoplasmic tail. What is apparent in these studies is that the recruitment of moesin, but not ezrin, to L-selectin tail requires PMA stimulation and that this recruitment can be prevented using an inhibitor of all known PKC isoforms, Ro

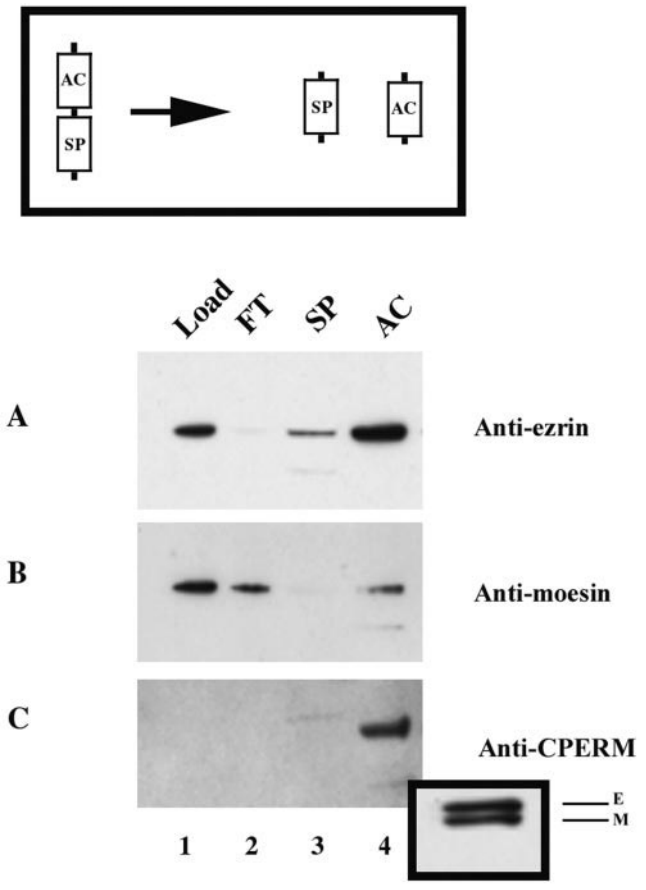

FIG. 5. **Specific enrichment of CPERM proteins by L-selectin tail.** *Schematic* at the *top* of the figure represents the order in which the columns were arranged and detached for subsequent elution. Extracts from PMA-stimulated lymphocytes were applied to a column construct containing the scrambled peptide stacked on top of the wild-type L-selectin tail column and washed extensively in 50 mM NaCl wash buffer. The columns were subsequently detached, and the affinity column was eluted using ethanolamine-based elution buffer. Both ezrin and moesin were detected in the starting material (*Load*), using polyclonal anti-ezrin and anti-moesin antibodies, respectively (*A* and *B, lane 1*). CPERM proteins are detected exclusively in fractions eluting from the affinity column (*C, lane 4*). *Inset* demonstrates that further resolution of *lane 4* identifies both the presence of moesin and ezrin (*E*, ezrin, and *M*, moesin). *FT*, flow-through; *SP*, scrambled peptide; *AC*, affinity column.

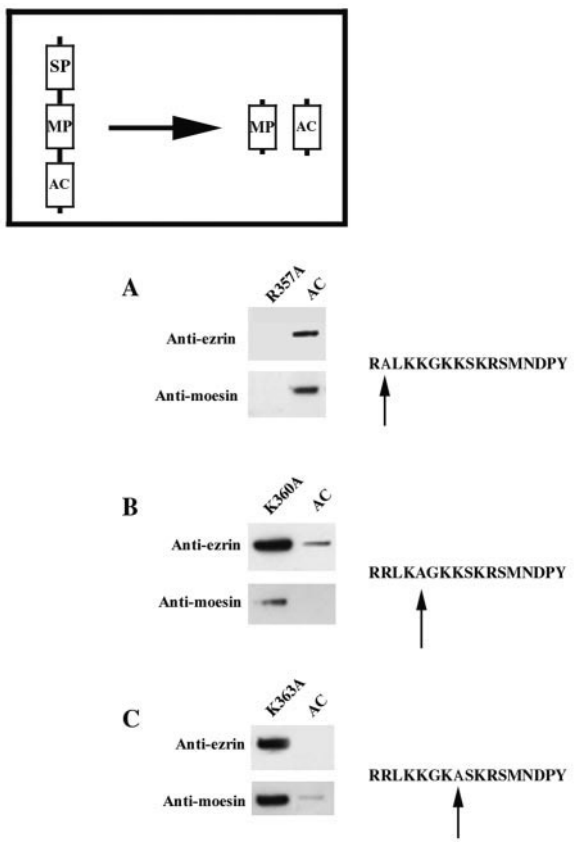

FIG. 6. **Alanine mutation of L-selectin cytoplasmic tail affects ERM protein binding.** PMA-stimulated lymphocytes were applied through three columns assembled in series (*i.e.* scrambled peptide column (*SP*), mutant peptide column (*MP*), and affinity column (*AC*), see *schematic* at *top* of figure). Columns were detached from one another and each subsequently eluted with 0.5 M ethanolamine. To the *right* of each set of immunoblots is the amino acid sequence of the various mutant L-selectin tails generated. The *arrow* indicates the position of the alanine mutation for each mutant peptide column. *A,* mutation R357A of L-selectin cytoplasmic tail abrogates binding of moesin and ezrin. Immunoblot analysis shows that moesin and ezrin eluted specifically from the affinity column. Both mutations K360A (*B*) and K363A (*C*) had no effect on either moesin or ezrin interaction with the cytoplasmic tail of L-selectin.

31-8220. Arginine 357 is essential for the association of both ezrin and moesin to L-selectin tail, suggesting that both interact with the membrane-proximal domain of L-selectin. Surface plasmon resonance studies clearly showed that N-terminal moesin and L-selectin tail interact specifically, with an approximate dissociation constant of 40 nM.

From rolling, to arrest, to chemotaxis, and trans-endothelial cell migration, the leukocyte is required to transform from a spherical to a polarized morphology during the different phases of the multistep adhesion cascade. Such dynamic changes in membrane morphology rely on rapid rearrangements of the cortical actin-based cytoskeleton. One group of proteins that mediate linkage between F-actin and the cell membrane are the ERM proteins. The ERM proteins are localized to the uropod (or trailing end) of activated leukocytes migrating toward a chemotactic source (20). Re-localization of cell adhesion molecules such as CD43, CD44, P-selectin glycoprotein ligand-1, intercellular adhesion molecule-2, and intercellular adhesion molecule-3 to the uropod of polarized leukocytes is orchestrated by the cytoskeleton, through interaction with ERM proteins. L-selectin, however, is rapidly shed from chemotactically activated leukocytes (21) and is therefore absent from uropods.

ERM proteins are highly related to one another, possessing over 85% sequence identity at their N termini, suggesting that they may be functionally redundant. Prevention of ERM protein expression in mouse thymoma cells using antisense oligonucleotides abolishes the formation of microvilli, highlighting their role in microvillus formation (22). Studies in moesin-deficient mice, however, reveal that microvilli on platelets appear normal and that no obvious phenotype exists in these mice, suggesting that ERM proteins may be functionally redundant (23). Earlier studies, however, indicate that although all three ERM proteins can be expressed in mammalian cultured cells, their expression patterns are restricted to certain adult tissues, suggesting that they serve specified roles (14). Indeed, we have observed that radixin is not expressed in murine lymphocytes, which is consistent with what has been documented previously (24) for human lymphocytes and platelets.

Although highly abundant, ERM proteins exist predominantly in a "dormant" cytosolic form, folded by intramolecular association of their N and C termini. Regulation of ERM function is controlled, in part, by phosphorylation. An as yet unidentified kinase phosphorylates ERM proteins at a critical C-terminal threonine residue. This leads to the disruption of the intramolecular interactions made between the N and C

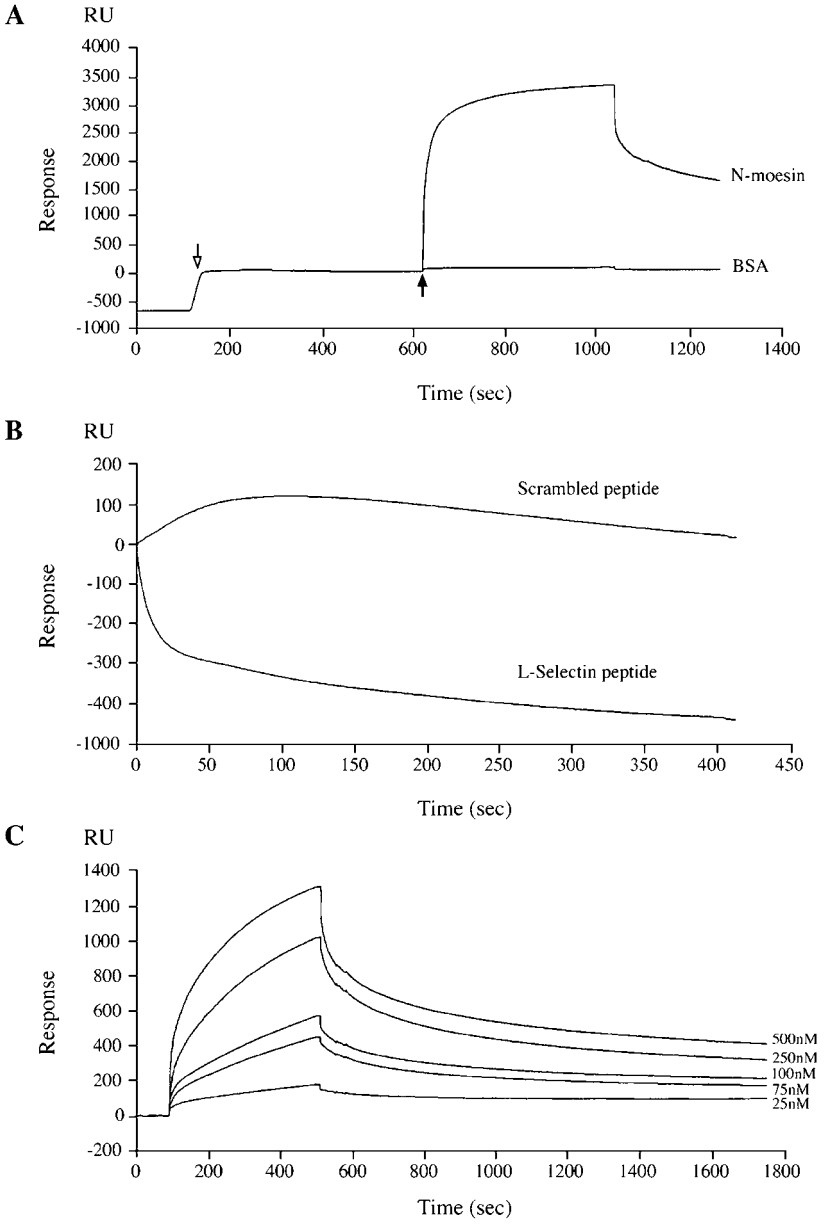

FIG. 7. **Direct interaction between the N-terminal domain of moesin and L-selectin cytoplasmic tail.** Surface plasmon resonance analysis of binding of purified (>99%) N-terminal domain of moesin with biotinylated L-selectin cytoplasmic tail, immobilized on streptavidin-coated sensorchips. *A,* immobilization of biotinylated L-selectin peptide on streptavidin sensor surface followed by association of 5 μM purified N-terminal moesin (*N-moesin*). No net nonspecific binding of 5 μM BSA to L-selectin cytoplasmic tail was observed. *Open arrow* denotes injection of biotinylated cytoplasmic tail, followed by a wash time of over 400 s at a flow rate of 5 μl/min. *Closed arrow* denotes the injection of either N-terminal moesin or BSA. *B,* binding of N-terminal moesin to immobilized L-selectin cytoplasmic tail peptide can be competed with the wild-type L-selectin peptide but not with a scrambled peptide (both injected at 100 μM). Sensogram displays the optical resonance during injection of peptides (normalized to zero). *C,* titration of N-terminal moesin against the immobilized L-selectin cytoplasmic tail. Association (100–500 s) and dissociation (500–1750 s) are shown.

termini, which in turn unfolds and activates ERM proteins. Several kinase activities have been implicated in facilitating the C-terminal threonine phosphorylation of ERM proteins, *e.g.* Rho kinase (15), PKCθ (25), PKCα (26), and phosphatidylinositol 4-phosphate 5-kinase (27). Such "ERM-activating kinases" may in fact be cell type-specific. Activation of ERM proteins leads to translocation from the cytosol to the cell membrane, allowing them to directly cross-link type I transmembrane proteins with F-actin via their N and C termini, respectively (28). ERM cross-linking of F-actin with the cell membrane is thought to facilitate the production of microvilli (29, 30) and other membrane structures, such as cleavage furrows (31) and membrane ruffles (32). ERM proteins generally associate with positively charged clusters of amino acids, located on membrane-proximal cytoplasmic domains of integral membrane proteins (16, 17). It is noteworthy that the membrane-proximal 5 amino acids of L-selectin tail (*i.e.* RRLKK) constitute an ideal ERM-binding motif. Moreover, an 11-amino acid truncation of human L-selectin tail clearly demonstrates that the first 6 amino acids of L-selectin tail (RRLKKG) is sufficient to anchor L-selectin to microvilli (3).

Previous reports documenting interactions between ERM proteins and cell adhesion molecules emphasize that the interaction is sensitive to NaCl (16, 33). We have similarly experienced sensitivity of ERM proteins binding to the L-selectin tail, where most of our washing conditions are sub-physiological ionic strengths. The use of phosphatidylinositol 4,5-bisphosphate has been shown to increase the ionic strength of interaction between ERM proteins and CD44 tail (33). Phosphatidylinositol 4,5-bisphosphate is considered to confer stability to activated ERM proteins, targeting them to the plasma membrane (34).

By using monoclonal antibody 297S, which exclusively detects activated CPERM proteins, we provide strong evidence that L-selectin tail specifically enriched for CPERM proteins. This interaction may not appear surprising as L-selectin is usually positioned on microvilli, and CPERM proteins are involved in the production of microvilli (16). One report (35) has documented the accumulation of L-selectin in cleavage furrows of dividing Daudi B-cell lymphomas, which are incidentally rich in ERM proteins (22, 36, 37). However, because the binding of ezrin and moesin to L-selectin tail differ with respect to

PMA stimulation, this suggests that the two proteins, although higly related, could be regulated differently. Based on this observation, we speculate that ezrin and moesin may regulate distinct aspects of L-selectin expression/function.

The fact that we observe ezrin interacting with L-selectin tail in the absence of PMA stimulation suggests that ezrin may be constitutively associated with L-selectin tail. Ezrin could therefore be involved in the constitutive anchoring of L-selectin to microvilli. Moesin, but not ezrin, however, is recruited to L-selectin tail exclusively under PMA-stimulating conditions, and this interaction can be significantly reduced using the PKC inhibitor, Ro 31-8220. Further analysis of total CPERM levels from lymphocyte extracts, pretreated with or without PMA, demonstrated that PMA did not alter the relative amounts of C-terminally phosphorylated ezrin or moesin. This observation suggests that the association of moesin with L-selectin tail could be regulated by a PKC-dependent factor(s), which either prevents or promotes C-terminally phosphorylated moesin from associating with L-selectin tail. It is also possible that moesin is phosphorylated on another residue(s), which cannot be detected by monoclonal antibody 297S, and that this other phosphorylation event may regulate the association of moesin with L-selectin tail.

Although we demonstrate here the physical interaction between L-selectin cytoplasmic tail and ERM proteins, the biological significance of this interaction remains unclear. Alanine mutation analysis of L-selectin tail revealed that arginine 357 is a critical residue for binding of both moesin and ezrin. Interestingly, this is at a region that is close to the putative calmodulin-binding site on human L-selectin (8). It would be interesting to assess whether there is any interplay between calmodulin and moesin with respect to L-selectin expression. PMA stimulation of human leukocytes leads to dissociation of calmodulin from L-selectin tail, which is in contrast to what we observe, using murine lymphocytes. We find that calmodulin appears to interact with L-selectin tail irrespective of PMA stimulation. This discrepancy could be due to the difference in methodologies used.

A recent report (38) demonstrates the efficiency of PMA-induced shedding of various cytoplasmic tail truncations of murine L-selectin. PMA-induced shedding of murine L-selectin containing the amino acids RRLKK in its cytoplasmic tail is almost as efficient as wild-type L-selectin. However, complete truncation of the cytoplasmic tail of L-selectin reduces the efficiency of PMA-induced shedding from 88 to 44%, further emphasizing the importance of the membrane-proximal cytoplasmic domain in PMA-induced L-selectin shedding. The idea that moesin may be involved in PMA-stimulated shedding is currently being addressed. Finally, perhaps once L-selectin is cleaved, the membrane-associated cleavage product is internalized and degraded, and this internalization process is mediated through moesin but not ezrin. It would be of interest to study the effects of L-selectin R357A on microvillar localization, rolling on L-selectin ligands, L-selectin shedding, its ability to act as a signaling receptor, and turnover of the cleaved membrane retained fragment. Studies using moesin-deficient mice may also shed light on the role of ERM proteins in regulating the function and/or expression of L-selectin. Such experiments may determine whether moesin and ezrin have overlapping or distinct roles in the lymphocyte.

Acknowledgments—We thank Clare Isacke, Steve Gamblin, Steve Smesdon, and Paul Thompson for helpful discussions. We are grateful to S. Tsukita and D. Sacks for generous gifts of anti-CPERM and anti-calmodulin antibodies and A. Bretscher for the kind gift of N-terminal moesin-expressing bacterial strain. We also thank Pete Fletcher and Steve Howell for synthesis of peptides and help with MALDI analysis, respectively.

REFERENCES

1. Gonzalez-Amaro, R., and Sanchez-Madrid, F. (1999) *Crit. Rev. Immunol.* **19,** 389–429
2. Springer, T. A. (1994) *Cell* **76,** 301–314
3. Pavalko, F. M., Walker, D. M., Graham, L., Goheen, M., Doerschuk, C. M., and Kansas, G. S. (1995) *J. Cell Biol.* **129,** 1155–1164
4. Kansas, G. S., Ley, K., Munro, J. M., and Tedder, T. F. (1993) *J. Exp. Med.* **177,** 833–838
5. Evans, S. S., Schleider, D. M., Bowman, L. A., Francis, M. L., Kansas, G. S., and Black, J. D. (1999) *J. Immunol.* **162,** 3615–3624
6. Stein, J. V., Cheng, G., Stockton, B. M., Fors, B. P., Butcher, E. C., and von Andrian, U. H. (1999) *J. Exp. Med.* **189,** 37–50
7. Springer, T. A. (1995) *Annu. Rev. Physiol.* **57,** 827–872
8. Kahn, J., Walcheck, B., Migaki, G. I., Jutila, M. A., and Kishimoto, T. K. (1998) *Cell* **92,** 809–818
9. Diaz-Rodriguez, E., Esparis-Ogando, A., Montero, J. C., Yuste, L., and Pandiella, A. (2000) *Biochem. J.* **346,** 359–367
10. Tsukita, S., and Yonemura, S. (1999) *J. Biol. Chem.* **274,** 34507–34510
11. Preece, G., Murphy, G., and Ager, A. (1996) *J. Biol. Chem.* **271,** 11634–11640
12. Reczek, D., Berryman, M., and Bretscher, A. (1997) *J. Cell Biol.* **139,** 169–179
13. Szabo, A., Stolz, L., and Granzow, R. (1995) *Curr. Opin. Struct. Biol.* **5,** 699–705
14. Bretscher, A., Chambers, D., Nguyen, R., and Reczek, D. (2000) *Annu. Rev. Cell Dev. Biol.* **16,** 113–143
15. Matsui, T., Maeda, M., Doi, Y., Yonemura, S., Amano, M., Kaibuchi, K., and Tsukita, S. (1998) *J. Cell Biol.* **140,** 647–657
16. Yonemura, S., Hirao, M., Doi, Y., Takahashi, N., Kondo, T., and Tsukita, S. (1998) *J. Cell Biol.* **140,** 885–895
17. Legg, J. W., and Isacke, C. M. (1998) *Curr. Biol.* **8,** 705–708
18. Merenmies, J., Pihlaskari, R., Laitinen, J., Wartiovaara, J., and Rauvala, H. (1991) *J. Biol. Chem.* **266,** 16722–16729
19. Wang, H., Bloom, O., Zhang, M., Vishnubhakat, J. M., Ombrellino, M., Che, J., Frazier, A., Yang, H., Ivanova, S., Borovikova, L., Manogue, K. R., Faist, E., Abraham, E., Andersson, J., Andersson, U., Molina, P. E., Abumrad, N. N., Sama, A., and Tracey, K. J. (1999) *Science* **285,** 248–251
20. Serrador, J. M., Nieto, M., and Sanchez-Madrid, F. (1999) *Trends Cell Biol.* **9,** 228–233
21. Kishimoto, T. K., Jutila, M. A., Berg, E. L., and Butcher, E. C. (1989) *Science* **245,** 1238–1241
22. Takeuchi, K., Sato, N., Kasahara, H., Funayama, N., Nagafuchi, A., Yonemura, S., and Tsukita, S. (1994) *J. Cell Biol.* **125,** 1371–1384
23. Doi, Y., Itoh, M., Yonemura, S., Ishihara, S., Takano, H., Noda, T., and Tsukita, S. (1999) *J. Biol. Chem.* **274,** 2315–2321
24. Shcherbina, A., Bretscher, A., Kenney, D. M., and Remold-O'Donnell, E. (1999) *FEBS Lett.* **443,** 31–36
25. Pietromonaco, S. F., Simons, P. C., Altman, A., and Elias, L. (1998) *J. Biol. Chem.* **273,** 7594–7603
26. Ng, T., Parsons, M., Hughes, W. E., Monypenny, J., Zicha, D., Gautreau, A., Arpin, M., Gschmeissner, S., Verveer, P. J., Bastiaens, P. I., and Parker, P. J. (2001) *EMBO J.* **20,** 2723–2741
27. Matsui, T., Yonemura, S., and Tsukita, S. (1999) *Curr. Biol.* **9,** 1259–1262
28. Gary, R., and Bretscher, A. (1995) *Mol. Biol. Cell* **6,** 1061–1075
29. Amieva, M. R., Wilgenbus, K. K., and Furthmayr, H. (1994) *Exp. Cell Res.* **210,** 140–144
30. Yonemura, S., and Tsukita, S. (1999) *J. Cell Biol.* **145,** 1497–1509
31. Yonemura, S., Nagafuchi, A., Sato, N., and Tsukita, S. (1993) *J. Cell Biol.* **120,** 437–449
32. Bretscher, A. (1989) *J. Cell Biol.* **108,** 921–930
33. Hirao, M., Sato, N., Kondo, T., Yonemura, S., Monden, M., Sasaki, T., Takai, Y., and Tsukita, S. (1996) *J. Cell Biol.* **135,** 37–51
34. Barret, C., Roy, C., Montcourrier, P., Mangeat, P., and Niggli, V. (2000) *J. Cell Biol.* **151,** 1067–1080
35. Po, J. L., Mak, A., Ginsberg, D., Huerta, P., Manoukian, R., Shustik, C., and Jensen, G. S. (1999) *Haematologica* **84,** 785–793
36. Kawano, Y., Fukata, Y., Oshiro, N., Amano, M., Nakamura, T., Ito, M., Matsumura, F., Inagaki, M., and Kaibuchi, K. (1999) *J. Cell Biol.* **147,** 1023–1038
37. Kosako, H., Yoshida, T., Matsumura, F., Ishizaki, T., Narumiya, S., and Inagaki, M. (2000) *Oncogene* **19,** 6059–6064
38. Zhao, L., Shey, M., Farnsworth, M., and Dailey, M. O. (2001) *J. Biol. Chem.* **276,** 30631–30640